

Determination of Tool Profile for the Milling of Three Screw Pump Rotor*

GIOVANNI MIMMI¹ and PAOLO PENNACCHI²

¹Università degli studi di Pavia, Dipartimento di Meccanica Strutturale, Via Ferrata 1, I-27100 Pavia, Italy

²Politecnico di Milano, Dipartimento di Meccanica, Piazza Leonardo da Vinci 32, I-20133 Milano, Italy

Abstract. The rotors of three screw pumps are commonly machined using shaped milling cutters. The determination of the exact shape of the cutter is very important, since a high precision in the machining is required to obtain a high volumetric efficiency of the pump. This paper describes a method to determine the theoretical shape of the cutter, starting from the characteristic parameters of the pump. The rotors are modeled in space by helicoids. Then, the contact line between the tool and the workpiece is determined and this allows us to define the exact cutter profile, with a suitable reference system transformation.

Sommario. I rotori delle pompe a tre viti vengono solitamente lavorati utilizzando frese di forma. La determinazione della forma esatta dei taglienti è molto importante, dato che una elevata precisione nella lavorazione è necessaria per ottenere un alto rendimento volumetrico della pompa. Questo lavoro descrive una metodologia per la determinazione del profilo teorico dell'utensile, partendo dai parametri caratteristici della pompa. I rotori vengono modellati nello spazio con superfici elicoidali. Si determina poi la linea lungo la quale l'utensile agisce sul pezzo e ciò permette, con un opportuno cambiamento del sistema di riferimento, di definire l'esatto profilo del tagliente.

Key words: Screw pumps, Tools profile determination, Shaped milling cutter, Applied mechanics.

Nomenclature

a - helix pitch;	p - parameter of screw;	β - angle subtended by epitrochoid or epicycloid arc;
a - auxiliary reference system index;	\mathbf{r} - surface vector;	Γ - line;
b - auxiliary reference system index;	r - central rotor inner radius, idler rotor outer radius;	γ - semiamplitude of not threaded zone of the screws;
c - tool index;	r_e - central rotor outer radius;	γ_c - tool setting angle;
e_c - distance of milling cutter center from the screw axis;	r_i - idler rotor inner radius;	\mathcal{G} - surface coordinate;
f - equation of meshing for a screw motion and surface;	S - reference system;	Ξ - solution locus of the screw equation of meshing;
f - reference system index;	s - screw index;	Σ - surface;
\mathbf{M} - transformation matrix;	T - definition set of the helicoid parameters;	ψ - angle between the screw and the reference frame.
\mathbf{N} - normal vector;	u - surface coordinate;	
N - normal vector component;		

1. Introduction

Three screw pumps have two types of rotors: a central screw, which presents two helical worms, and two identical idler rotors, driven by the central and with two corresponding helical vanes.

The machining technology is the same for both rotors: starting from the solid piece, the rotors are usually cut by shaped milling cutters.

However, for our purposes it is not necessary to give a complete topological representation of the milling cutter identifying each tooth. The only important thing is the cutter radial section; so we can consider a simplified tool comparable to a disk grinding wheel from a geometrical point of view. The disk, if that is the case, can be machined to obtain the usual milling cutter, but this phase is not interesting here, since it is a standard methodology in tool production.

2. Mathematical model

The method (see Figure 1) introduced in this paper starts from the analytical description of the screws in the space, which are modeled as helicoid surfaces. The kinematic analysis is omitted here since it is reported in [1]. Stated the cut parameters, the equation of meshing, introduced by Litvin [2], allows to determine the contact line between the tool and the workpiece and eventually the tool shape by a suitable reference system transformation.

* Extended version of a communication presented at the *Joint Conference of Italian Group of Computational Mechanics and Ibero-Latin American Association of Computational Methods in Engineering*, September 25-27, 1996, Padova, Italy.

It is necessary to observe that also Henriot [3] and other authors proposed methods to determine the cutter theoretical section, but Litvin's [2] method has been preferred, even with some modifications, since it seems more general and complete.

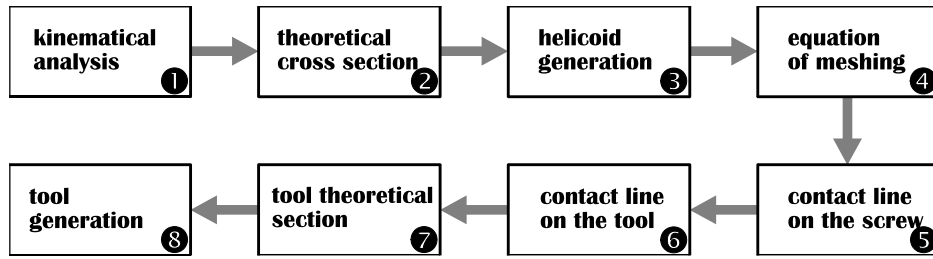


Figure 1 - Flow chart of the method.

The modeling and relative calculations have been done by using many programs written with symbolic mathematics software [4]. Many figures have been made by this software and refer, except when specified, to a particular case, characterized by the following parameters: $r = 12$ mm, $r_e = 20$ mm, $a = 68$ mm, $\gamma = 45^\circ$, $\gamma_c = 48^\circ 3'$, $e_c = (50 + r)$ mm for the central screw and $e_c = (50 + r_i)$ mm for the idler.

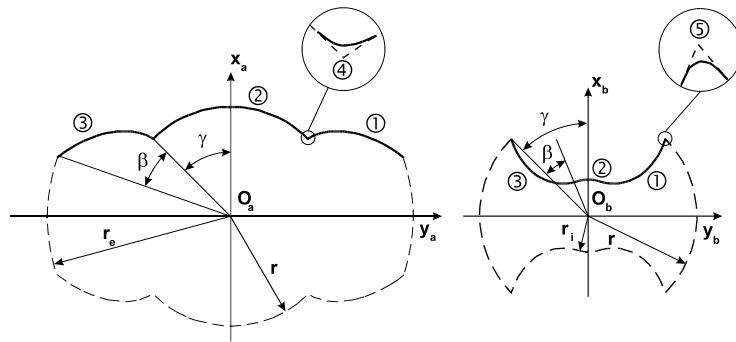


Figure 2 - Cross section of the rotors: central rotor (left), idler rotor (right).

2.1. HELICOIDS REPRESENTATION

In the first part of the proposed method it is necessary to refer to some considerations expressed in [1] about the screw profile generation on a cross section to the rotating axis (1 and 2 in Figure 1). In this paragraph we wish to give a mathematical model that defines the screw surface in three dimensional space (3 in Figure 1) that is composed of several helicoid surfaces in an analytical representation. Figure 2 shows the cross section of the two types of rotors under consideration. The solid lines numbered from 1 to 3 represent the three parts of the profile machined by the milling cutter.

If we refer to the two auxiliary reference systems $O_a x_a y_a$ and $O_b x_b y_b$ (these are left hand systems due to the choice of the reference system S_s in Figure 4), the flanks that have to be considered are respectively epicycloid and root circle (equal to the pitch circle) arc for the central screw and epitrochoid and root circle arc for the idler. Their parametric equations are:

$$\begin{cases} x_{a1,3} = 2r \cos(\vartheta_{1,3} + \gamma) - r \cos(2\vartheta_{1,3} + \gamma) \\ y_{a1,3} = \pm 2r \sin(\vartheta_{1,3} + \gamma) \mp r \sin(2\vartheta_{1,3} + \gamma) \\ z_{a1,3} = 0 \end{cases} \quad T_{1,3}: 0 \leq \vartheta_{1,3} \leq \arccos \frac{5r^2 - r_e^2}{4r^2} \quad (1)$$

$$\begin{cases} x_{a2} = r \cos(-\vartheta_2 + \gamma) \\ y_{a2} = r \sin(-\vartheta_2 + \gamma) \\ z_{a2} = 0 \end{cases} \quad T_2: 0 \leq \vartheta_2 \leq 2\gamma \quad (2)$$

$$\begin{cases} x_{b1,3} = 2r \cos(\vartheta_{1,3} - \gamma + \beta) - r_e \cos(2\vartheta_{1,3} - \gamma + \beta) \\ y_{b1,3} = \mp 2r \sin(\vartheta_{1,3} - \gamma + \beta) \pm r_e \sin(2\vartheta_{1,3} - \gamma + \beta) \\ z_{b1,3} = 0 \end{cases} \quad T_{1,3}: 0 \leq \vartheta_{1,3} \leq \arccos \frac{3r^2 + r_e^2}{4rr_e} \quad (3)$$

$$\begin{cases} x_{b2} = (2r - r_e) \cos(-\vartheta_2 + \gamma - \beta) \\ y_{b2} = -(2r - r_e) \sin(-\vartheta_2 + \gamma - \beta) \\ z_{b2} = 0 \end{cases} \quad T_2: 0 \leq \vartheta_2 \leq 2(\gamma - \beta). \quad (4)$$

In the previous equations, T_i are the definition intervals and β the angle subtended by epitrochoid or epicycloid arc (see Figure 2). Using a vector notation the equations (1)-(4) can be rewritten as

$$\mathbf{r}_{ai} = [x_{ai} \quad y_{ai} \quad z_{ai} \quad 1]^T \text{ and } \mathbf{r}_{bi} = [x_{bi} \quad y_{bi} \quad z_{bi} \quad 1]^T \text{ with } i = 1, 2, 3. \quad (5)$$

The helicoid is generated by each flank with a screw motion along its z axis. The transformation matrix is (for a right-hand screw):

$$\mathbf{M} = \begin{bmatrix} \cos u_s & -\sin u_s & 0 & 0 \\ \sin u_s & \cos u_s & 0 & 0 \\ 0 & 0 & 1 & p u_s \\ 0 & 0 & 0 & 1 \end{bmatrix}. \quad (6)$$

The parameter p is linked to the helix pitch a by the relationship

$$p = \frac{a}{2\pi}. \quad (7)$$

Therefore the surfaces Σ_{si} that represent the machined surfaces of the screws are given by the following vectorial equations, where the index (c) is relative to the central rotor and (i) to the idler rotor:

$$\mathbf{r}_{si}^{(c)} = \mathbf{M} \mathbf{r}_{ai} \text{ with } i = 1, 2, 3 \quad (8)$$

$$\mathbf{r}_{si}^{(i)} = \mathbf{M} \mathbf{r}_{bi} \text{ with } i = 1, 2, 3. \quad (9)$$

From equations (8) and (9) we can obtain the parametric expressions of the surfaces Σ_{si} as function of the surface coordinates u_s and ϑ_s :

$$\begin{cases} x_{s1,3}^{(c)}(u_s, \vartheta_{s1,3}) = 2r \cos(\vartheta_{s1,3} \pm u_s + \gamma) - r \cos(2\vartheta_{s1,3} \pm u_s + \gamma) \\ y_{s1,3}^{(c)}(u_s, \vartheta_{s1,3}) = \pm 2r \sin(\vartheta_{s1,3} \pm u_s + \gamma) \mp r \sin(2\vartheta_{s1,3} \pm u_s + \gamma) \\ z_{s1,3}^{(c)}(u_s, \vartheta_{s1,3}) = p u_s \end{cases} \quad T_{1,3}: \begin{cases} 0 \leq \vartheta_{s1,3} \leq \arccos \frac{5r^2 - r_e^2}{4r^2}, \\ -\pi \leq u_s \leq \pi \end{cases} \quad (10)$$

$$\begin{cases} x_{s2}^{(c)}(u_s, \vartheta_{s2}) = r \cos(-\vartheta_{s2} - u_s + \gamma) \\ y_{s2}^{(c)}(u_s, \vartheta_{s2}) = r \sin(-\vartheta_{s2} - u_s + \gamma) \\ z_{s2}^{(c)}(u_s, \vartheta_{s2}) = p u_s \end{cases} \quad T_2: \begin{cases} 0 \leq \vartheta_{s2} \leq 2\gamma, \\ -\pi \leq u_s \leq \pi \end{cases} \quad (11)$$

$$\begin{cases} x_{s1,3}^{(i)}(u_s, \vartheta_{s1,3}) = 2r \cos(\vartheta_{s1,3} \mp u_s - \gamma + \beta) - r_e \cos(2\vartheta_{s1,3} \mp u_s - \gamma + \beta) \\ y_{s1,3}^{(i)}(u_s, \vartheta_{s1,3}) = \mp 2r \sin(\vartheta_{s1,3} \mp u_s - \gamma + \beta) \pm r_e \sin(2\vartheta_{s1,3} \mp u_s - \gamma + \beta) \\ z_{s1,3}^{(i)}(u_s, \vartheta_{s1,3}) = p u_s \end{cases} \quad T_{1,3}: \begin{cases} 0 \leq \vartheta_{s1,3} \leq \arccos \frac{3r^2 + r_e^2}{4rr_e}, \\ -\pi \leq u_s \leq \pi \end{cases} \quad (12)$$

$$\begin{cases} x_{s2}^{(i)}(u_s, \vartheta_{s2}) = (2r - r_e) \cos(\vartheta_{s2} + u_s - \gamma + \beta) \\ y_{s2}^{(i)}(u_s, \vartheta_{s2}) = (2r - r_e) \sin(\vartheta_{s2} + u_s - \gamma + \beta) \\ z_{s2}^{(i)}(u_s, \vartheta_{s2}) = p u_s \end{cases} \quad T_2: \begin{cases} 0 \leq \vartheta_{s2} \leq 2(\gamma - \beta), \\ -\pi \leq u_s \leq \pi \end{cases} \quad (13)$$

The choice of the limits for the surface coordinate u_s is rather arbitrary. With the suggested choice, it is possible to obtain a helicoid as long as a pitch. Previous equations (10)-(13) allow us to generate the complete helicoid in space. This helicoid represents the considered screws, together with the other surfaces which compose the screw and which have not been analytically represented because they are not necessary in what follows. In Figure 3 the two screws are shown; note that the central screw is right-handed, whereas the idler is left-handed. To obtain the latter, it is sufficient to change the sign of u_s in the upper left submatrix in (6), relative to the rotation part of the transformation matrix \mathbf{M} . In

the following, the equations for right-handed screws will always be considered, because the worm winding direction is indifferent to the determination of the milling cutter profile.

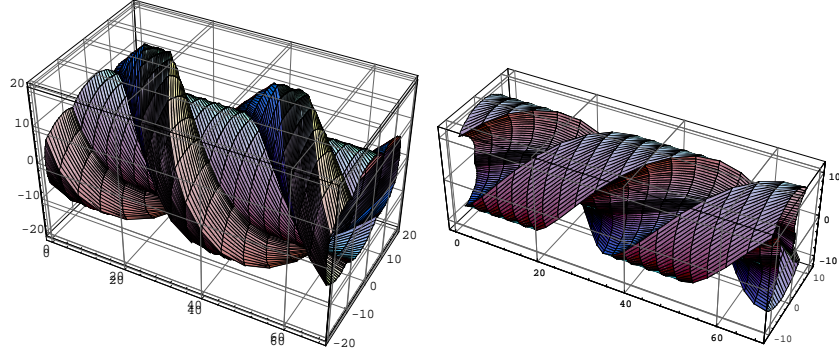


Figure 3 - Central screw (left) - idler screw (right).

2.2. REFERENCE SYSTEMS

Figure 4 shows a draft relative to the reference systems adopted. Since we often shift from one reference system to the other, it is advisable to examine them briefly. The reference system S_f is a fixed reference system $O_f x_f y_f z_f$ rigidly connected to the machine tool frame.

The reference system S_s represents a reference system $O_s x_s y_s z_s$ rigidly connected to the screw, which performs a screw motion relative to the fixed along the common axis $z_f \equiv z_s$. In the general instant t , the origin O_s will be shifted relative to O_f of $p\psi$, while the axes x_s and y_s make the angle ψ with the corresponding axes x_f and y_f . The reference system S_c ($O_c x_c y_c z_c$) is rigidly connected to the tool. The distance from the milling cutter center O_c to the axis $z_f \equiv z_s$, indicated by e_c , is one of the most important cut parameters, together with the angle γ_c , which is the tool setting angle relative to the fixed reference system.

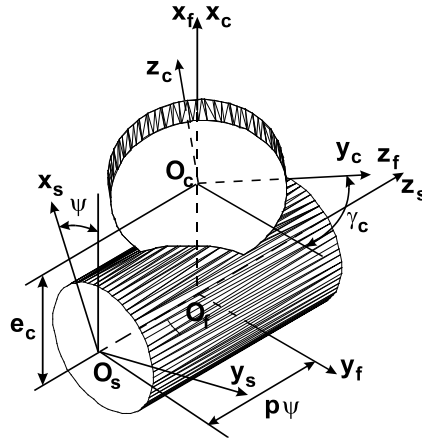


Figure 4 - Frame, tool, screw reference systems.

It is practical to use the notation \mathbf{M}_{ab} for the transformation matrixes, which indicates the transformation matrix from the reference system S_b to S_a . Referring to Figure 4, we have

$$\mathbf{M}_{fc} = \begin{bmatrix} 1 & 0 & 0 & e_c \\ 0 & \cos \gamma_c & -\sin \gamma_c & 0 \\ 0 & \sin \gamma_c & \cos \gamma_c & 0 \\ 0 & 0 & 0 & 1 \end{bmatrix} \quad (14)$$

$$\mathbf{M}_{fs} = \begin{bmatrix} \cos \psi & -\sin \psi & 0 & 0 \\ \sin \psi & \cos \psi & 0 & 0 \\ 0 & 0 & 1 & p\psi \\ 0 & 0 & 0 & 1 \end{bmatrix} \quad (16)$$

$$\mathbf{M}_{cf} = \mathbf{M}_{fc}^{-1} = \begin{bmatrix} 1 & 0 & 0 & -e_c \\ 0 & \cos \gamma_c & \sin \gamma_c & 0 \\ 0 & -\sin \gamma_c & \cos \gamma_c & 0 \\ 0 & 0 & 0 & 1 \end{bmatrix} \quad (15)$$

$$\mathbf{M}_{sf} = \mathbf{M}_{fs}^{-1} = \begin{bmatrix} \cos \psi & \sin \psi & 0 & 0 \\ -\sin \psi & \cos \psi & 0 & 0 \\ 0 & 0 & 1 & -p\psi \\ 0 & 0 & 0 & 1 \end{bmatrix} \quad (17)$$

2.3 EQUATION OF MESHING

The equation of meshing, proposed by Litvin [2] for the case of conjugate surfaces, but which is also suitable for a couple composed of a tool and the generated workpiece, represents the necessary condition for the existence of the envelope of a conjugate surface to a given one. Considering the tool and the workpiece, it is obvious that the latter is determined by the envelope of the tool in subsequent positions, but it is also evident that the example can be reversed and the workpiece can be considered as enveloping the tool.

The equation of meshing (4 in Figure 1) permits us to determine a relationship between the values of the surface coordinates u_s and ϑ_s , in order to define the line along which a surface meshes with its conjugate surface. In the case of the couple workpiece-tool, the line obtained as a function of the solution locus of the equation of meshing represents the line on the workpiece where the tool cuts.

For the determination of the equation of meshing, Litvin states this theorem [2]: “the line of tangency between screw surface Σ_s and tool surface Σ_c is such a one at which the normals to screw surface Σ_s intersect the rotation axis of the tool” (z_c in Figure 4). The proof of this theorem is rather intuitive, considering that tool surface Σ_c is a surface of revolution and therefore the normal to each point intersects the fixed axis. So also the normal to the screw at the point where its surface Σ_s is tangent to that of the tool (that is where the cutting action takes place) intersects the fixed axis of the tool.

Therefore it is necessary to determine the normal to the screw surface Σ_s first, then its intersection with the tool axis is imposed and sets the relationship between the surface coordinates u_s and ϑ_s .

This method is used for all three surfaces Σ_{si} that have to be machined for each screw. In order to reduce the length of this exposition, we are introducing a general type of notation to refer to a generic surface \mathbf{r}_s such as

$$\mathbf{r}_s = \mathbf{r}_s(u_s, \vartheta_s) = [x_s(u_s, \vartheta_s) \quad y_s(u_s, \vartheta_s) \quad z_s(u_s, \vartheta_s) \quad 1]^T \quad (18)$$

where the equations (10)-(13) have to replace the functions x_s, y_s, z_s . Since all the equations (10)-(13) are $C^\infty(\mathbf{T})$ in their surface coordinate definition sets, the surfaces under consideration have the normal at every point given by

$$\mathbf{N}_s = \begin{vmatrix} \mathbf{i} & \mathbf{j} & \mathbf{k} \\ \frac{\partial x_s}{\partial u_s} & \frac{\partial y_s}{\partial u_s} & \frac{\partial z_s}{\partial u_s} \\ \frac{\partial x_s}{\partial \vartheta_s} & \frac{\partial y_s}{\partial \vartheta_s} & \frac{\partial z_s}{\partial \vartheta_s} \end{vmatrix} = N_{xs}(u_s, \vartheta_s)\mathbf{i}_s + N_{ys}(u_s, \vartheta_s)\mathbf{j}_s + N_{zs}(u_s, \vartheta_s)\mathbf{k}_s. \quad (19)$$

The normal common to screw surface Σ_s and tool surface Σ_c is given in Cartesian coordinates:

$$\frac{X_s - x_s(u_s, \vartheta_s)}{N_{xs}(u_s, \vartheta_s)} = \frac{Y_s - y_s(u_s, \vartheta_s)}{N_{ys}(u_s, \vartheta_s)} = \frac{Z_s - z_s(u_s, \vartheta_s)}{N_{zs}(u_s, \vartheta_s)} \quad (20)$$

In equation (20) X_s, Y_s, Z_s represent the coordinates of the intersection point P of the normal and the tool axis z_c in the screw reference system S_s . If we consider the particular position with $\psi = 0$, the screw reference coincides with the fixed reference, the P coordinates in S_c are transformed into S_s reference system with the following:

$$\begin{bmatrix} X_s \\ Y_s \\ Z_s \\ 1 \end{bmatrix} = \mathbf{M}_{sf} \mathbf{M}_{fc} \begin{bmatrix} 0 \\ 0 \\ Z_c \\ 1 \end{bmatrix} = \begin{bmatrix} e_c \\ -Z_c \sin \gamma_c \\ Z_c \cos \gamma_c \\ 1 \end{bmatrix}. \quad (21)$$

Substituting equation (21) in equation (20), we have

$$\frac{e_c - x_s(u_s, \vartheta_s)}{N_{xs}(u_s, \vartheta_s)} = \frac{-Z_c \sin \gamma_c - y_s(u_s, \vartheta_s)}{N_{ys}(u_s, \vartheta_s)} = \frac{Z_c \cos \gamma_c - z_s(u_s, \vartheta_s)}{N_{zs}(u_s, \vartheta_s)}. \quad (22)$$

Equation (22) is already the equation of meshing. By eliminating Z_c we have

$$(e_c - x_s) \cos \gamma_c N_{ys}^2 + (y_s \cos \gamma_c - z_s \sin \gamma_c) N_{xs} N_{ys} + (e_c - x_s) \sin \gamma_c N_{ys} N_{zs} + 2 y_s \sin \gamma_c N_{xs} N_{zs} = 0. \quad (23)$$

Equation (23) can be further simplified by considering that the relation exists for the helicoids [2]:

$$y_s N_{xs} - x_s N_{ys} - p N_{zs} = 0. \quad (24)$$

Finally we have

$$f(u_s, \vartheta_s) = (e_c - x_s + p \cot \gamma_c) N_{zs} + e_c \cot \gamma_c N_{ys} + z_s N_{xs} = 0 \quad (25)$$

which is the equation of meshing for the helicoids in the commonly known form. The couples of values $(\bar{u}_s, \bar{\vartheta}_s)$ that satisfy equation (25) define a curve Ξ in the u_s, ϑ_s plane.

2.4. CONTACT LINES ON THE SCREWS

A set of contact lines (\bullet in Figure 1) exists on the screw surface. We will consider just one: Γ , as shown in Figure 5 by imposing $\psi = 0$ and having the fixed reference system S_f and the screw reference S_s coincide.

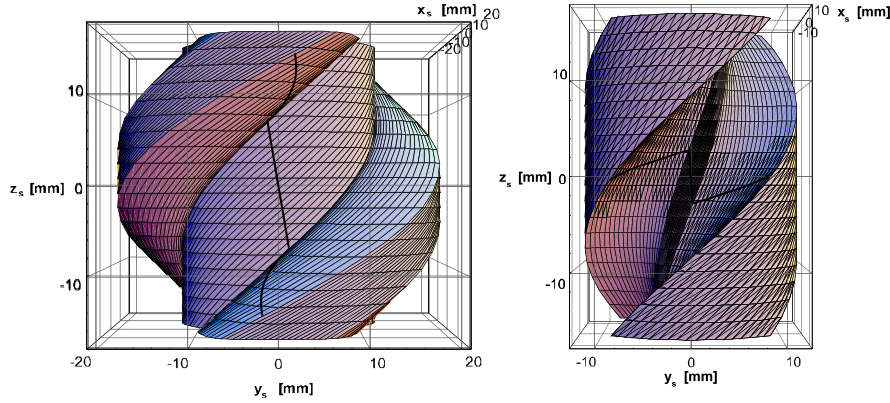


Figure 5 - Contact lines on the screw surfaces.

So the contact line Γ_s which is actually composed of three lines per each machined surface for both the screws, has the equation

$$\Gamma_s \begin{cases} \mathbf{r}_s = \mathbf{r}_s(u_s, \vartheta_s) = x_s(u_s, \vartheta_s) \mathbf{i}_s + y_s(u_s, \vartheta_s) \mathbf{j}_s + z_s(u_s, \vartheta_s) \mathbf{k}_s \\ f(u_s, \vartheta_s) = 0 \end{cases} \quad (26)$$

If angle ψ is varied, the subsequent contact lines will sweep out the surface of the screw. As a result of the previous considerations, line Γ is common to the tool. In reference system S_c its equation is given by

$$\Gamma_c \begin{cases} \mathbf{r}_c = \mathbf{M}_{cf} \mathbf{M}_{fs} \mathbf{r}_s(u_s, \vartheta_s) \\ f(u_s, \vartheta_s) = 0 \end{cases} \quad (27)$$

Before showing the contact lines for the tool, it would be best to design it completely.

2.5. TOOL CUTTING EDGE

It is unnecessary to give a complete topological representation of the milling cutter. The only important thing is the cutter shape so we consider a simplified tool comparable to a disk grinding wheel (see Figure 6) from which each cutter is obtained. Therefore our particular tool is a solid of revolution that is obtained by rotating a cutter profile on plane $x_c z_c$ about z_c axis. The equations that define the section (\bullet in Figure 1) can be obtained by equation (27). By considering that it represents Γ_c in space, and rotating each point of Γ_c into $x_c z_c$ plane of cutter reference system S_c we have:

$$\begin{cases} x_c^{sct} = -\sqrt{x_c^2(\bar{u}_s, \bar{\vartheta}_s) + y_c^2(\bar{u}_s, \bar{\vartheta}_s)} \\ z_c^{sct} = z_c(\bar{u}_s, \bar{\vartheta}_s) \end{cases} \text{ where } (\bar{u}_s, \bar{\vartheta}_s) \in \Xi. \quad (28)$$

In equation (28) we have chosen the negative abscissas half plane because that section is directly in contact with the workpiece according to the reference systems in Figure 4. Note that it is possible to prove that equation (27) can be expressed as function of just one parameter. In fact the two parameters u_s and ϑ_s are not independent, but related by equation (25), and we can prove that a function $\vartheta_s = \vartheta_s(u_s)$ exists that is implicitly defined by equation (25) in a sufficient small region of each point $(\bar{u}_s, \bar{\vartheta}_s) \in \Xi$. It is possible to show, using Dini's theorem [5], that the equation of meshing (25) gives a unique solution, so it is possible to express the equation in explicit form, that is $\vartheta_s = \vartheta_s(u_s)$. In fact all the following hypotheses are true:

- $f(u_s, \vartheta_s)$ of equation (25) is continuous in each point of T_i sets of equations (10)-(13);
- the partial derivative $f_{\vartheta_s}(u_s, \vartheta_s)$ exists;
- the root $(\bar{u}_s, \bar{\vartheta}_s)$ exists due to the previous considerations;
- it is possible to verify that $f_{\vartheta_s}(\bar{u}_s, \bar{\vartheta}_s) \neq 0$.



Figure 6 - Simplified tool like a shaped grinding wheel.

Therefore the equation (28) can be rewritten as

$$\begin{cases} x_c^{sct}(u_s) = -\sqrt{x_c^2(u_s, \vartheta_s(u_s)) + y_c^2(u_s, \vartheta_s(u_s))} \\ z_c^{sct}(u_s) = z_c(u_s, \vartheta_s(u_s)) \end{cases} \quad (29)$$

where $u_s \in \Xi'$, that is to the subset of Ξ just composed by the values \bar{u}_s .

The theoretical shapes of the cutter on a radial section for both the screws are reported in Figure 7.

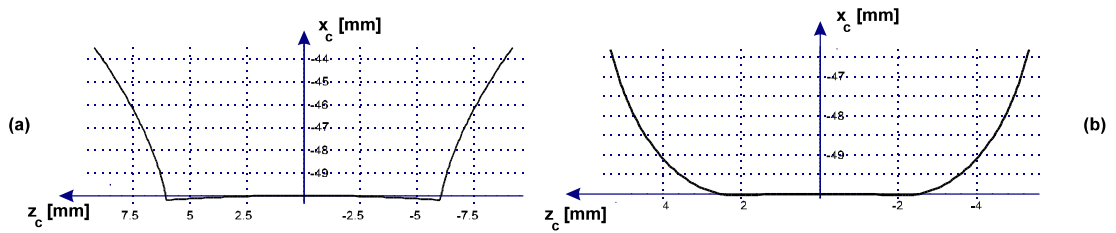


Figure 7 - Theoretical tool radial section for central screw (a), idler screw (b).

The theoretical profiles have been compared with those of actual tools as shown in Figure 8, where the solid white line represents the theoretical profile. The differences on the top of the central screw tool (A-A' in Figure 8) are due to the impossibility to maintain the sharp edge in the points A-A' during the machining. Considering the idler screw tool, notice the straight fillet (C-D in Figure 8), that does not contribute to the cut if suitably chosen, and the fillet on the bottom (B-C in Figure 8). This represents a technological necessity to blunt the edges on the tips of the idler screw (see ⑤ in Figure 2), that must not interfere with the fillet on the pitch circle of the central screw (see ④ in Figure 2). This fillet is unavoidable due to the wear on the top of the milling cutter.

The surface of revolution (③ in Figure 1), that represents the tool, is given by the following vector, obtained by imposing the rotation of the curve of equation (29) that is the tool axial profile

$$\mathbf{r}_c^{tool}(u_s, \vartheta_c) = \begin{bmatrix} \cos \vartheta_c & -\sin \vartheta_c & 0 & 0 \\ \sin \vartheta_c & \cos \vartheta_c & 0 & 0 \\ 0 & 0 & 1 & 0 \\ 0 & 0 & 0 & 1 \end{bmatrix} \begin{bmatrix} x_c^{sct}(u_s) \\ 0 \\ z_c^{sct}(u_s) \\ 1 \end{bmatrix} = x_c^{sct}(u_s) \cos \vartheta_c \mathbf{i}_c + x_c^{sct}(u_s) \sin \vartheta_c \mathbf{j}_c + z_c^{sct}(u_s) \mathbf{k}_c \quad (30)$$

where $u_s \in \Xi'$ and $\vartheta_c \in [-\pi, \pi]$.

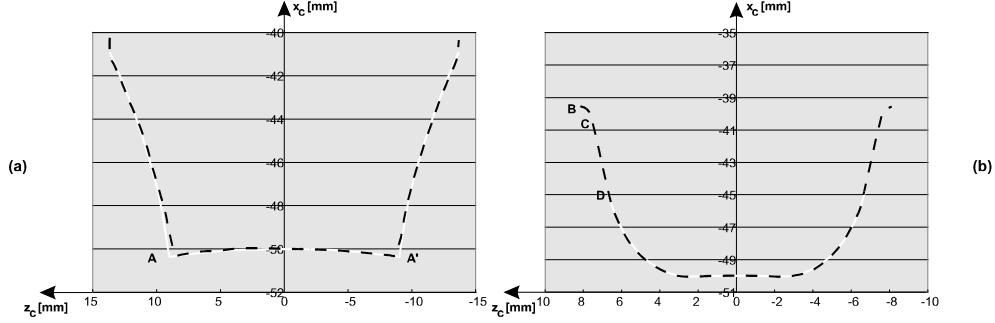


Figure 8 - Comparison between a theoretical tool (white solid line) and actual (black dashed line) of rotors with $r = 33$ mm, $r_e = 55$ mm, $a = 86$ mm, $\gamma = 49^\circ$, $\gamma_c = 39^\circ 40'$; (a) central, (b) idler.

The solid black line in Figure 9 is the contact line on a tool surface sector, while Figure 10 shows a 3D image of a theoretical milling cutter complete of teeth, whose cutter profile has been determined with the method here introduced.

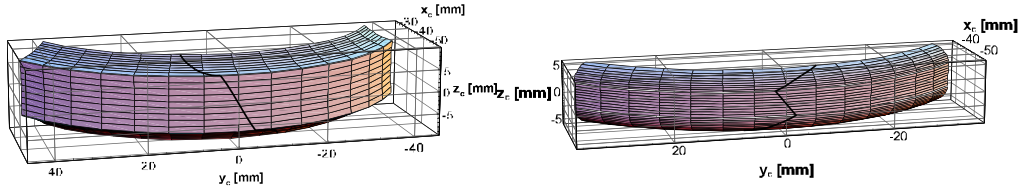


Figure 9 - Contact lines on the tool for the central rotor screw (left) and for the idler rotor screw (right).

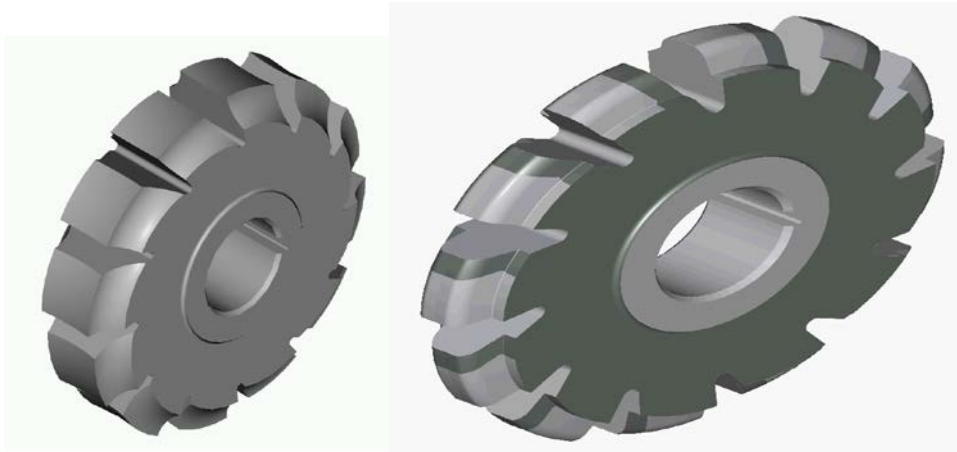


Figure 10 - 3D rendered milling cutters: central screw (left), idler screw (right).

3. Conclusions

In this paper we have shown a mathematical model to define surfaces that represent the rotors of screw pumps in the Cartesian space. These surfaces are helicoids that have a suitable analytical representation. Starting from this mathematical model, we use the equation of meshing algorithm to find the relation between the surface coordinates and determine the contact line between the tool and the screw to be machined.

The contact line in the tool reference system allows us to determine the section of the cutter and the surface of revolution that can represent the theoretical tool. These results may give the basis for further studies on the influence of the tool sharpening on the shape of the machined rotors.

Acknowledgment

The research was made thanks to a contribution of M.U.R.S.T.

References

1. Mimmi, G., Pennacchi, P., 1995, 'Design of three-screw positive displacement rotary pumps', proceedings of *Contact Mechanics II-Computational Techniques*, 11-13 july 1995, Ferrara, Italy;
2. Litvin, F.L., 1994, *Gear Geometry and Applied Theory*, Prentice Hall, Englewood Cliffs, NJ;
3. Henriot, G., 1979, *Ingranaggi - Trattato Teorico Pratico*, vol.2, Tecniche Nuove, Milano;
4. Wolfram, S., 1991, *Mathematica*, 2 ed., Addison Wesley Publishing Co., Redwood City, CA;
5. Amerio, L., 1985, *Analisi Matematica*, vol.2, UTET, Torino.